# New Travelling Wave Solutions for an Asymmetric Model of a Rod in a Lattice Fluid with Nonlinear Advection

Sayed A. Elwakil<sup>a</sup>, Mohsen A. Zahran<sup>a</sup>, Refaat Sabry<sup>b</sup>, and Emad K. El-Shewy<sup>a</sup>

<sup>a</sup> Theoretical Physics Group, Physics Department, Faculty of Science, Mansoura University, Mansoura, Egypt

<sup>b</sup> Theoretical Physics Group, Physics Department, Faculty of Science, Mansoura University, New Damietta 34517, Damietta, Egypt

Reprint requests to M. A. Z.; E-mail: m\_zahran1@mans.edu.eg

Z. Naturforsch. 61a, 430-438 (2006); received May 29, 2006

Based on the modified extended tanh-function method, we consider the continuum problem of the driven diffusive flow of particles behind an impenetrable obstacle (rod) of the length L. The results show that the presence of an obstacle, whether stationary or moving, in a driven diffusive flow with nonlinear drift will distort the local concentration profile to a state which divided the (x,y)-plane into two regions. The concentration is relatively higher in one side than the other side, apart from the value of  $\frac{D}{vL}$ , where D is the diffusion coefficient and v is the drift velocity. This problem has relevance for the size segregation of particulate matter which results from the relative motion of different-size paricles induced by shaking. The obtained soultions include soliton, periodical, rational and singular solutions

Key words: Lattice Fluid Models; Diffusion-Advection Processes; Modified Extended tanh-Function Method; Symbolic Computations.

### 1. Introduction

As is well-known, many important phenomena and dynamical processes in physics and related sciences are described by nonlinear partial differential equations (NPDEs). One of these phenomena is the size segregation of particulate matter produced by shaking, which is important in many industrial situations such as in powder separation by the vibration of a non-uniform mixture [1].

In an effort to better understand the dynamics of the segregation process, the dynamical picture of this phenomena was modeled by Rosato et al. [1,2] where they considered a two-dimensional system of large and small disks of equal masses. The disks were subjected to a gravitational force in the vertical direction and interact with each other and with the walls of their container through a hard-core potential. Computer simulations gave results consistent with the experiments; after many shakes, the larger disks lie on the top of smaller ones in a nonequilibrium stationary state. Later, Alexander and Lebowitz [3] investigated the driven diffusive motion of a polymer in a sea of monomers where the particles move on a lattice subjected to a driving field that biases jump rates in

a direction perpendicular to the polymer which occupies L sites (monomers occupy one sites). Then, computer simulations of a two-dimensional square lattice of a polymer-monomer lattice system showed the unexpected behavior that the polymer velocity v(L) (as a function of its length L) first decreases and then increases. Also, in [4] a model consists of a gas of monomers and a single rod on a lattice was considered. A monomer occupies one site and the rod more than one site. The computer simulations in [4] showed a surprising relationship between the rod's velocity and its length in the stationary state; beyond a certain length, the longer rods moved faster, although more sites need to be empty in order for longer rods to move. This unexpected behavior led Alexander and Lebowitz [4] to study the probability that all of the sites next to the right of the rod were simultaneously unoccupied. Then they showed that the long rods, whether stationary or moving, distort the local monomer profile to a state which is independent of the monomer density and create a larger depletion region to the right of them.

For the seek of a better understanding of the asymmetrical interacting particle model with two kinds of particles, Alexander and Lebowitz [4] have presented a detailed description of some related continuum models

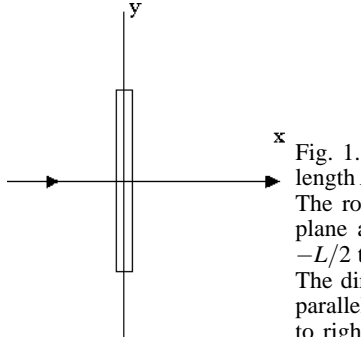


Fig. 1. An obstacle (rod), of length L, parallel to the z-axis. The rod intersects the (x,y)-plane along the interval y = -L/2 to y = L/2 on the axis. The direction of advection is parallel to the x-axis from left to right (the moving fram of the rod).

whose behavior is quite similar to that of the particle model. They introduced the continuum model

$$u_t = D(u_{xx} + u_{yy}) - v u_x, \tag{1}$$

where the flux of particles in the fluid consists of a diffusive part -Du(x, y, t) and a linear drift part vu(x, y, t), where u(x, y, t) is the particle concentration, D the diffusion coefficient, and v the drift velocity. In the steady state, (1) was studied by Philip et al. [5], who were considering the flow of ground water around a cylindrical obstacle. They obtained an exact solution in the form of an infinite series. In [4], it was stated that the solution given in [5] has the qualitative features of the density profile and resembles at observed in the computer simulations of monomer flow behind a stationary obstacle. The same problem was cosidered by Knessl and Keller [6]. They considered the effect of an impenetrable obstacle upon the concentration of the particles in a fluid when the particles moved by diffusion and linear advection.

In [7], the classical Lie group method was used for studying another model of the driven diffusive flow whose behaviour is quite similar to that of a rod in a lattice fluid given in [4]. Following [4,7] and using the modified extended tanh-function (METF) method [8-10], we will consider the continuum problem of the driven diffusive flow of particles behind an impenetrable strip of the length L which is parallel to the z-axis. The strip is centered in the origin and normal to the incident flow which takes the direction parallel to the x-axis from left to right (as shown in Fig. 1). The flux of particles in the fluid is composed of row tends: a linear diffusive term  $-Du_{y}$  perpendicular to the nonlinear drift tend vLk(u), where u(x,y,t) is the particle concentration, D the diffusion coefficient, v the drift velocity, and k(u) a nonlinear function of the particle

concentration. We further impose that there can be no flux through the length L of the strip. The velocity v may result from the motion of the fluid (advection), or from the gravitional field acting on the particles (drift). Conservation of particles implies that the divergence of the flux equals to  $-u_t$ . Therefore, when D and v are constants, u(x, y, t) satisfies the nonlinear diffusionadvection equation in (2+1) dimension

$$u_t = D u_{yy} - v L[K(u)]_x. \tag{2}$$

In fact, when K(u) equals  $\frac{1}{L}u(1-u)$ , then (2) reduces to the continuum model suggested in [4] [i. e. (16)], while for the case K(u) = u(1-u), (2) reduces to the case studied in [7] using the classical Lie group method which is a very complicated mathematical technique see for example [7, 11–13]. In (2), we will examine (analytically) the existence of travelling wave solutions for the following two cases: (i)  $K(u) = u^m$ , where  $m \neq 0, 1$  (i.e. the fact that m is an arbitrary will enable us to see the effect of the nonlinear drift), and (ii) K(u) = u(1-u).

This paper is organized as follows. In Section 2, a summary of the METF method is introduced. In Section 3, the METF method is applied to (2), where the above two cases are considered. A discussion will be presented in Section 4.

## 2. Summary of the METF Method

Consider a given NPDE with one physical field u(x,y,t) in three variables x, y and t:

$$H(u, u_t, u_x, u_y, u_{xt}, u_{yt}, u_{xy}, u_{xx}, u_{xy}, u_{yy}, \dots) = 0.$$
 (3)

We seek its special solution, i. e. travelling wave solution, in the form

$$u(x,t) = u(\zeta), \quad \zeta = x + y - \lambda t,$$

where  $\lambda$  is a constant to be determined later. Then, (3) will be reduced to a nonlinear ordinary differential equation. The next crucial step is that the solution we are looking for is expressed in the form

$$u(\zeta) = \sum_{i=0}^{n} a_i \omega^i + \sum_{i=1}^{n} b_i \omega^{-i}, \tag{4}$$

and

$$\omega' = k + \omega^2,\tag{5}$$

where k is a parameter to be determined,  $\omega = \omega(\zeta)$ ,  $\omega' = \frac{d\omega}{d\zeta}$ . Since, the underlying mechanism for solitary wave solutions to occur is the fact that different effects (such as dispersion, dissipation, and nonlinearity) that act to change the wave forms in many nonlinear physical equations have to balance out. Therefore, one may use the above fact to determine the parameter n which must be a positive integer and can be found by balancing the highest-order linear term with the nonlinear terms [14-17]. Substitution of (4) and (5) into the relevant ordinary differential equation will yield a system of algebraic equations with respect to  $a_0$ ,  $a_i$ ,  $b_i$ , k, and  $\lambda$  (where i = 1, ..., m) because all the coefficients of  $\omega^{j}$  (where  $j=0,1,\ldots,m$ ) have to vanish. With the aid of *Mathematica*, one can determine  $a_i$ ,  $b_i$ , k and  $\lambda$ . The Riccati equation (5) has the general solutions

$$\omega = \begin{cases} -\sqrt{-k} \tanh[\sqrt{-k}\zeta], & \text{with } k < 0, \\ -\sqrt{-k} \coth[\sqrt{-k}\zeta], & \text{with } k < 0, \end{cases}$$
 (6)

$$\omega = -\frac{1}{\zeta}, \quad \text{with } k = 0, \tag{7}$$

and

$$\omega = \begin{cases} \sqrt{k} \tan[\sqrt{k}\zeta], & \text{with } k > 0, \\ -\sqrt{k} \cot[\sqrt{k}\zeta], & \text{with } k > 0. \end{cases}$$
(8)

In fact, the METF method is limited to certain classes of NPDEs. However, it is an easy and direct method to obtain travelling wave solutions. Since, instead of solving a NPDE we will deal with a system of algebraic equations which can be handled by symbolic computation packages like *Maple* or *Mathematica*. It is clear that the METF method permits the following types of solutions: rational, triangular, singular and solitary wave solutions.

# 3. Explicit Exact Solutions for the Nonlinear Diffusion-Advection Equation in (2+1) Dimensions

Two cases of K(u) will be considered. **Case (i):**  $K(u) = u^m$  where  $m \neq 0, 1$ .

Then, (2) reduces to

$$u_t = Du_{vv} - vLmu^{m-1}u_x. (9)$$

Introducing the transformation  $u(x,y,t) = u(\zeta)$ , where  $\zeta = x + y + \lambda t$  into (9) leads to the ordinary differential equation

$$-\lambda u' + Du'' - \alpha m u^{m-1} u' = 0, \tag{10}$$

where  $\alpha = vL$ . Balancing u'' with  $u^{m-1}u'$  leads to  $n = \frac{1}{m-1}$ . Hence, we use the transformation

$$u = \vartheta^{\frac{1}{m-1}}. (11)$$

Substituting (11) into (10), we get

$$\alpha m(m-1) \vartheta^2 \vartheta' + D(m-2)(\vartheta')^2 + (m-1)(\lambda \vartheta' - D \vartheta'') \vartheta = 0.$$
(12)

Again, using the balance concept leads to

$$\vartheta(\zeta) = a_0 + \omega(a_1 + b_1 \omega^{-2}). \tag{13}$$

Substituting (13) into (12) and making use of (5), we get a system of algebraic equations for  $a_0$ ,  $a_1$ ,  $b_1$ , k, m, and  $\lambda$ :

$$(m-1)(ka_1-b_1) \left(\alpha m a_0^2 + \lambda a_0\right) - (m-2) D b_1^2$$

$$+ka_1^2 [Dk(m-2) + m(m-1) \alpha b_1] - m \alpha (m-1) a_1 b_1^2$$

$$-4 (2m-3) Dk b_1 a_1 = 0,$$

$$k(m-1)[\lambda a_1 - 2(D - m\alpha a_1)(a_0)]a_1 = 0,$$

$$-2Dka_1^2 + 6Db_1a_1 + m[-4D + (m-1)\alpha a_1]b_1a_1$$

$$(m-1)[m\alpha a_0^2 + km\alpha a_1^2 + a_0\lambda]a_1 = 0,$$

$$(m-1)[\lambda a_1 - 2(D - m\alpha a_1)a_0]a_1 = 0,$$

$$m[-D + (m-1)\alpha a_1]a_1^2 = 0,$$

$$(m-1)[\lambda b_1 + 2a_0(Dk + m\alpha b_1)]b_1 = 0,$$

$$b_1k[\alpha m(m-1)a_0^2 + 2Dk(2m-3)a_1$$

$$+(m-1)\lambda a_0] + [2D + \alpha m(m-1)a_1]kb_1^2$$

$$+\alpha m(m-1)b_1^3 = 0,$$

$$k(m-1)[\lambda b_1 + 2a_0(Dk + m\alpha b_1)]b_1 = 0,$$

and

$$km[Dk + \alpha(m-1)b_1]b_1^2 = 0.$$

Solving, with the aid of *Mathematica*, the above system of algebraic equations then nine different cases are obtained.

Case 1:

$$m = 2$$
,  $D = \alpha a_1$ ,  $\lambda = -2 \alpha a_0$ ,  
 $k = -\frac{b_1}{a_1}$ , where  $\alpha \neq 0$  and  $a_1 \neq 0$ . (14)

Case 2:

$$m=2, \quad D=\alpha a_1, \quad \lambda=-2\alpha a_0,$$
  
 $b_1=0, \quad \text{where } \alpha \neq 0 \text{ and } a_1 \neq 0.$  (15)

(24)

Case 3

$$m = \frac{4}{3}, D = \frac{\alpha a_1}{3}, b_1 = 0, \lambda = \mp 2i\sqrt{k}\alpha a_1,$$
 (16)  
 $a_0 = \pm i\sqrt{k}a_1$ , where  $\alpha \neq 0$  and  $a_1 \neq 0$ .

Case 4:

$$m = 2$$
,  $D = -\frac{\alpha b_1}{k}$ ,  $\lambda = -2 \alpha a_0$ ,  
 $a_1 = 0$ , where  $\alpha \neq 0, b_1 \neq 0$ , and  $k \neq 0$ . (17)

Case 5:

$$m = \frac{4}{3}, \ D = \frac{\alpha a_1}{3}, \ k = -\frac{b_1}{a_1}, \ \lambda = \mp 4 \alpha \sqrt{a_1 b_1},$$
 $a_0 = \pm 2 \sqrt{a_1 b_1}, \text{ where } \alpha \neq 0, a_1 \neq 0, \text{ and } b_1 \neq 0.$ 
(18)

Case 6:

$$m = \frac{4}{3}, D = -\frac{\alpha b_1}{3k}, a_1 = 0, \lambda = \mp \frac{2i \alpha b_1}{\sqrt{k}},$$
  
 $a_0 = \pm i \frac{b_1}{\sqrt{k}}, \text{ where } \alpha \neq 0, k \neq 0, \text{ and } b_1 \neq 0.$  (19)

Case 7:

$$D = (m-1) \alpha a_1, \ a_0 = \pm i \sqrt{k} a_1, \ \lambda = \mp 2i \sqrt{k} \alpha a_1,$$

$$b_1 = 0, \text{ where } m \neq 0, 1, 2, \frac{4}{3}, \alpha \neq 0, \text{ and } a_1 \neq 0.$$
(20)

Case 8:

$$D = (m-1) \alpha a_1, \quad a_0 = \pm 2 \sqrt{a_1 b_1},$$

$$\lambda = \mp 4 \alpha \sqrt{a_1 b_1}, \quad k = -\frac{b_1}{a_1}, \quad \text{where}$$

$$m \neq 0, 1, 2, \frac{4}{3}, \alpha \neq 0, a_1 \neq 0, \text{ and } b_1 \neq 0.$$
(21)

Case 9:

$$D = -\frac{\alpha (m-1)b_1}{k}, \quad a_0 = \pm i \frac{b_1}{\sqrt{k}},$$

$$\lambda = \mp \frac{2i \alpha b_1}{\sqrt{k}}, \quad a_1 = 0, \quad \text{where}$$

$$m \neq 0, 1, 2, \frac{4}{3}, \alpha \neq 0, k \neq 0, \text{ and } b_1 \neq 0.$$
(22)

Using the above 9 cases and making use of (13) and (11), one gets the correponding solutions for (9).

According to case 1, we have three different types of travelling wave solutions for *u*:

*Type 1*: for k = 0

$$u(x,y,t) = a_0 - \frac{D}{vL\zeta}, \quad \zeta = x + y + \lambda t,$$
 where  $\lambda = -2vLa_0$ . (23)

*Type 2*: for k < 0

$$\begin{split} u(x,y,t) = & a_0 - \frac{D\sqrt{-k}}{vL}\{\tanh[\sqrt{-k}\zeta] + \coth[\sqrt{-k}\zeta]\}, \\ \text{where } \zeta = & x + y + \lambda t \text{ and } \lambda = -2vLa_0. \end{split}$$

*Type 3*: for k > 0

$$u(x, y, t) = a_0 + \frac{D\sqrt{k}}{vL} \{ \tan[\sqrt{k}\zeta] - \cot[\sqrt{k}\zeta] \},$$
 where  $\zeta = x + y + \lambda t$  and  $\lambda = -2vLa_0$ . (25)

In solutions (23)–(25), m = 2,  $vL \neq 0$ ,  $D \neq 0$ , and  $a_0$  is an arbitrary constant.

Case 2 leads to the following three different types: *Type 1*: for k = 0

$$u(x,y,t) = a_0 - \frac{D}{vL\zeta}, \quad \zeta = x + y + \lambda t,$$
 where  $\lambda = -2vLa_0$ . (26)

*Type 2*: for k < 0

$$u(x,y,t) = a_0 - \frac{D\sqrt{-k}}{vL} \tanh[\sqrt{-k}\zeta],$$
where  $\zeta = x + y + \lambda t$  and  $\lambda = -2vLa_0$ . (27)

*Type 3*: for k > 0

$$u(x,y,t) = a_0 + \frac{D\sqrt{k}}{vL} \tan[\sqrt{k}\zeta],$$
 where  $\zeta = x + y + \lambda t$  and  $\lambda = -2vLa_0$ . (28)

In solutions (26)–(28), m = 2,  $vL \neq 0$ , and  $D \neq 0$ .

Case 3 results in:

Type 1: for k = 0

$$u(x,y,t) = -\left[\frac{3D}{vL(x+y)}\right]^3.$$
 (29)

*Type 2*: for k < 0

$$u(x,y,t) = \left[ \pm i \frac{3D\sqrt{-k}}{vL} - \frac{3D\sqrt{-k}}{vL} \tanh[\sqrt{-k}\zeta] \right]^3,$$

where  $\zeta = x + y + \lambda t$  and  $\lambda = \mp 6D\sqrt{-k}$ .

(30)

*Type 3*: for k > 0

$$u(x,y,t) = \left[\pm i \frac{3D\sqrt{k}}{vL} + \frac{3D\sqrt{k}}{vL} \tan[\sqrt{k}\zeta]\right]^{3},$$
 (31) where  $\zeta = x + y + \lambda t$  and  $\lambda = \mp 6iD\sqrt{k}$ .

In solutions (29)–(31),  $m = \frac{4}{3}$ ,  $vL \neq 0$ , and  $D \neq 0$ . Case 4 yields two different types:

*Type 1*: for k < 0

$$u(x,y,t) = a_0 - \frac{D\sqrt{-k}}{vL} \coth[\sqrt{-k}\zeta],$$
 where  $\zeta = x + y + \lambda t$  and  $\lambda = -2vLa_0$ . (32)

Type 2: for k > 0

$$u(x,y,t) = a_0 - \frac{D\sqrt{k}}{vL} \cot[\sqrt{k}\zeta],$$
 where  $\zeta = x + y + \lambda t$ , and  $\lambda = -2vLa_0$ . (33)

In solutions (32) and (33), m = 2,  $vL \neq 0$ , and  $D \neq 0$ . Case 5 yields two different types:

*Type 1*: for k < 0

$$u(x, y, t) = \left[\frac{3D\sqrt{-k}}{vL} \left(\pm 2 - \coth[\sqrt{-k}\zeta] - \tanh[\sqrt{-k}\zeta]\right)\right]^{3},$$
where  $\zeta = x + y + \lambda t$  and  $\lambda = \mp 12D\sqrt{-k}$ . (34)

*Type 2*: for k > 0

$$u(x,y,t) = \left[\frac{3D\sqrt{k}}{vL} \left(\pm 2i - \cot[\sqrt{k}\zeta] + \tan[\sqrt{k}\zeta]\right)\right]^{3},$$
where  $\zeta = x + y + \lambda t$  and  $\lambda = \mp 12D\sqrt{-k}$ .

Case 6 leads to:

*Type 1*: for k < 0

$$u(x,y,t) = \left[\frac{3D\sqrt{-k}}{vL} \left(\mp 1 - \coth[\sqrt{-k}\zeta]\right)\right]^3,$$
 (36) where  $\zeta = x + y + \lambda t$  and  $\lambda = \pm 6D\sqrt{-k}$ .

*Type 2*: for k > 0

$$u(x,y,t) = \left[\frac{3D\sqrt{k}}{vL} \left(\mp i - \cot[\sqrt{k}\zeta]\right)\right]^{3},$$
where  $\zeta = x + y + \lambda t$  and  $\lambda = \pm 6iD\sqrt{k}$ .

Solutions (34) – (37) are applicable for  $m = \frac{4}{3}$ ,  $vL \neq 0$  and  $D \neq 0$ .

Case 7 leads to:

*Type 1*: for k < 0

$$u(x,y,t) = \left[\frac{D\sqrt{-k}}{vL(m-1)} \left(\pm 1 - \tanh[\sqrt{-k}\zeta]\right)\right]^{\frac{1}{m-1}},$$
where  $\zeta = x + y + \lambda t$  and  $\lambda = \frac{\mp 2D\sqrt{-k}}{m-1}.$ 

Type 2: for k > 0

$$u(x,y,t) = \left[\frac{D\sqrt{k}}{vL(m-1)} \left(\pm i + \tan[\sqrt{k}\zeta]\right)\right]^{\frac{1}{m-1}},$$
where  $\zeta = x + y + \lambda t$  and  $\lambda = \frac{\mp 2iD\sqrt{k}}{m-1}$ . (39)

Type 3: for k = 0

$$u(x, y, t) = \left[\frac{-D}{vL(m-1)(x+y)}\right]^{\frac{1}{m-1}}.$$
 (40)

Case 8 yields two different types:

*Type 1*: for k < 0

$$u(x,y,t) = \left[\frac{D\sqrt{-k}}{vL(m-1)} \left(\pm 2 - \coth[\sqrt{-k}\zeta] - \tanh[\sqrt{-k}\zeta]\right)\right]^{\frac{1}{m-1}},$$
where  $\zeta = x + y + \lambda t$  and  $\lambda = \mp 4 \frac{D\sqrt{-k}}{(m-1)}$ .
$$(41)$$

*Type 2*: for k > 0

$$u(x,y,t) = \left[ \frac{D\sqrt{k}}{vL(m-1)} \left( \pm 2i - \cot[\sqrt{k}\zeta] + \tan[\sqrt{k}\zeta] \right) \right]^{\frac{1}{m-1}},$$
 (42) where  $\zeta = x + y + \lambda t$  and  $\lambda = \mp 4i \frac{D\sqrt{k}}{(m-1)}$ .

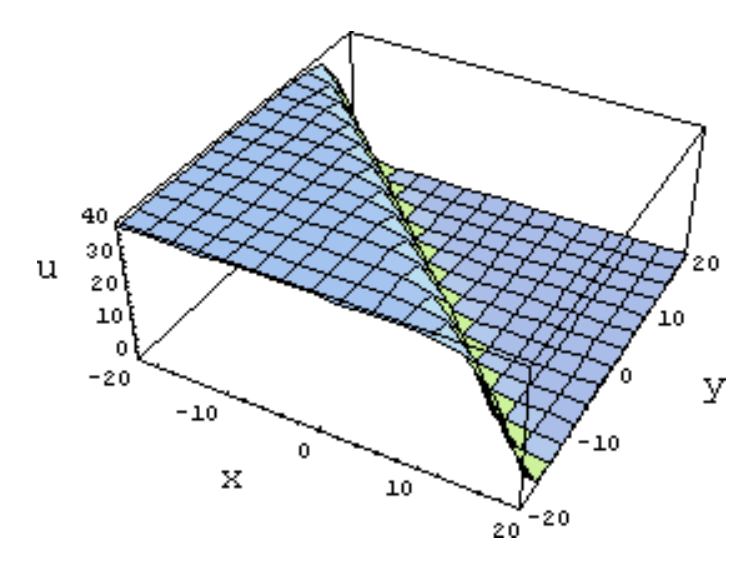


Fig. 2. Plot of the concentration u(x,y,t) for t = 0.001, D = 0.25, L = 0.1, v = 0.5, k = -0.1, and m = 3/2.

Finally, case 9 leads to:

*Type 1*: for k < 0

$$u(x,y,t) = \left[\frac{D\sqrt{-k}}{vL(m-1)}\left(\mp 1 - \coth[\sqrt{-k}\zeta]\right)\right]^{\frac{1}{m-1}}, \quad (43)$$
 where  $\zeta = x + y + \lambda t$  and  $\lambda = \pm 2\frac{D\sqrt{-k}}{(m-1)}$ .

*Type 2*: for k > 0

$$u(x, y, t) =$$

$$\left[\frac{D\sqrt{k}}{vL(m-1)}\left(\mp i - \cot[\sqrt{k}\zeta]\right)\right]^{\frac{1}{m-1}},$$
where  $\zeta = x + y + \lambda t$  and  $\lambda = \pm 2i\frac{D\sqrt{k}}{(m-1)}$ . (44)

Solutions (38) – (44) are valid under the conditions that  $vL \neq 0$ ,  $D \neq 0$  and  $m \neq 0, 1, 2, \frac{4}{3}$ .

**Case (ii):** K(u) = u(1 - u).

Then, (2) reduces to

$$u_t = D u_{yy} - v L [u(1-u)]_x.$$
 (45)

Introducing the transformation  $u(x,y,t) = u(\zeta)$ , where  $\zeta = x + y + \lambda t$  into (45) leads to the ordinary differential equation

$$-\lambda u' + Du'' - vL(1 - 2u)u' = 0. \tag{46}$$

Balancing the highest-order linear terms and nonlinear terms leads to

$$u(\zeta) = a_0 + \omega(a_1 + b_1 \omega^{-2}). \tag{47}$$

Substituting (47) into (45) and making use of (5), a system of algebraic equations for  $a_0$ ,  $a_1$ ,  $b_1$ , k, and  $\lambda$  is obtained:

$$(ka_1 - b_1)(\lambda + Lv - 2Lva_0) = 0,$$

$$ka_1(D + Lva_1) = 0,$$

$$a_1(\lambda + Lv - 2Lva_0) = 0,$$

$$a_1(D + Lva_1) = 0,$$

$$b_1(Dk - Lvb_1) = 0,$$

$$kb_1(\lambda + Lv - 2Lva_0) = 0,$$

and

$$kb_1(Dk-Lvb_1)=0,$$

from which, we find

$$D = -Lva_1, \quad \lambda = Lv(-1+2a_0), \quad b_1 = 0, \quad (48)$$

$$D = \frac{Lvb_1}{k}, \quad \lambda = Lv(-1+2a_0),$$

$$a_1 = 0, \quad k \neq 0,$$

$$(49)$$

and

$$D = \frac{Lvb_1}{k}, \quad \lambda = Lv(-1 + 2a_0),$$

$$a_1 = -\frac{b_1}{k}, \quad k \neq 0, \quad L \neq 0, \quad v \neq 0.$$
(50)

Due to (48), for k < 0 the solution to (45) reads

$$u(x, y, t) = a_0 + \frac{D}{Lv} \sqrt{-k} \tanh[\sqrt{-k}\zeta],$$
where  $\zeta = x + y + \lambda t$  and  $\lambda = Lv(-1 + 2a_0)$ , (51)

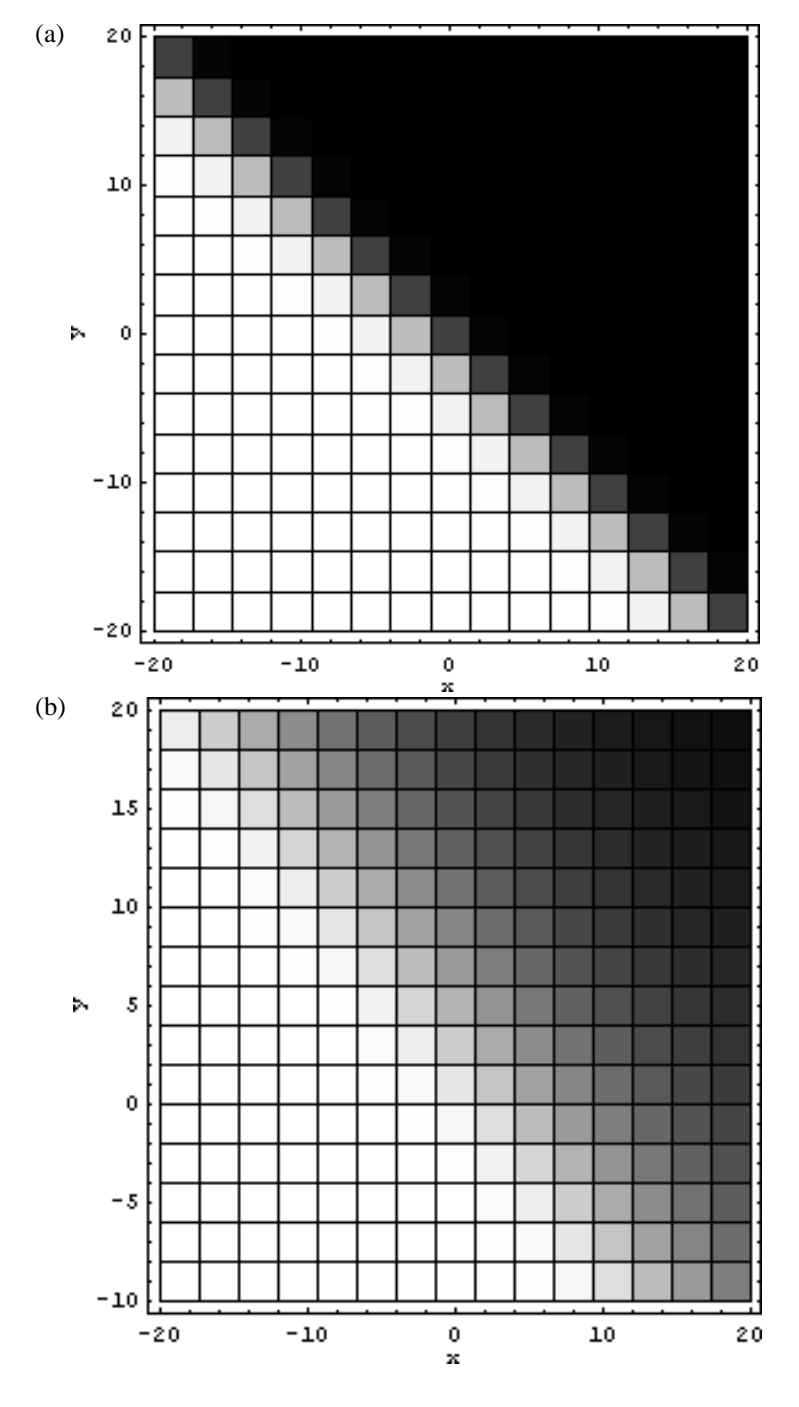


Fig. 3. Density plot of the concentration u(x,y,t), where regions in white mean u=0, while for black regions  $u \neq 0$  and u increases as the black gets darker, for  $t=0.001,\ D=0.25,\ L=0.1,\ v=0.5,\ k=-0.1$ , and (a) m=3/2 and (b) m=10.

while for k > 0 it is

and k and  $a_0$  are arbitrary constants. In the case k = 0, (48) leads to

$$u(x,y,t) = a_0 - \frac{D}{Lv}\sqrt{k}\tan[\sqrt{k}\zeta], \qquad u(x,y,t) = a_0 + \frac{D}{Lv}\frac{1}{\zeta},$$
 where  $\zeta = x + y + \lambda t$  and  $\lambda = Lv(-1 + 2a_0)$ , where  $\zeta = x + y + \lambda t$  and  $\lambda = Lv(-1 + 2a_0)$ . (53)

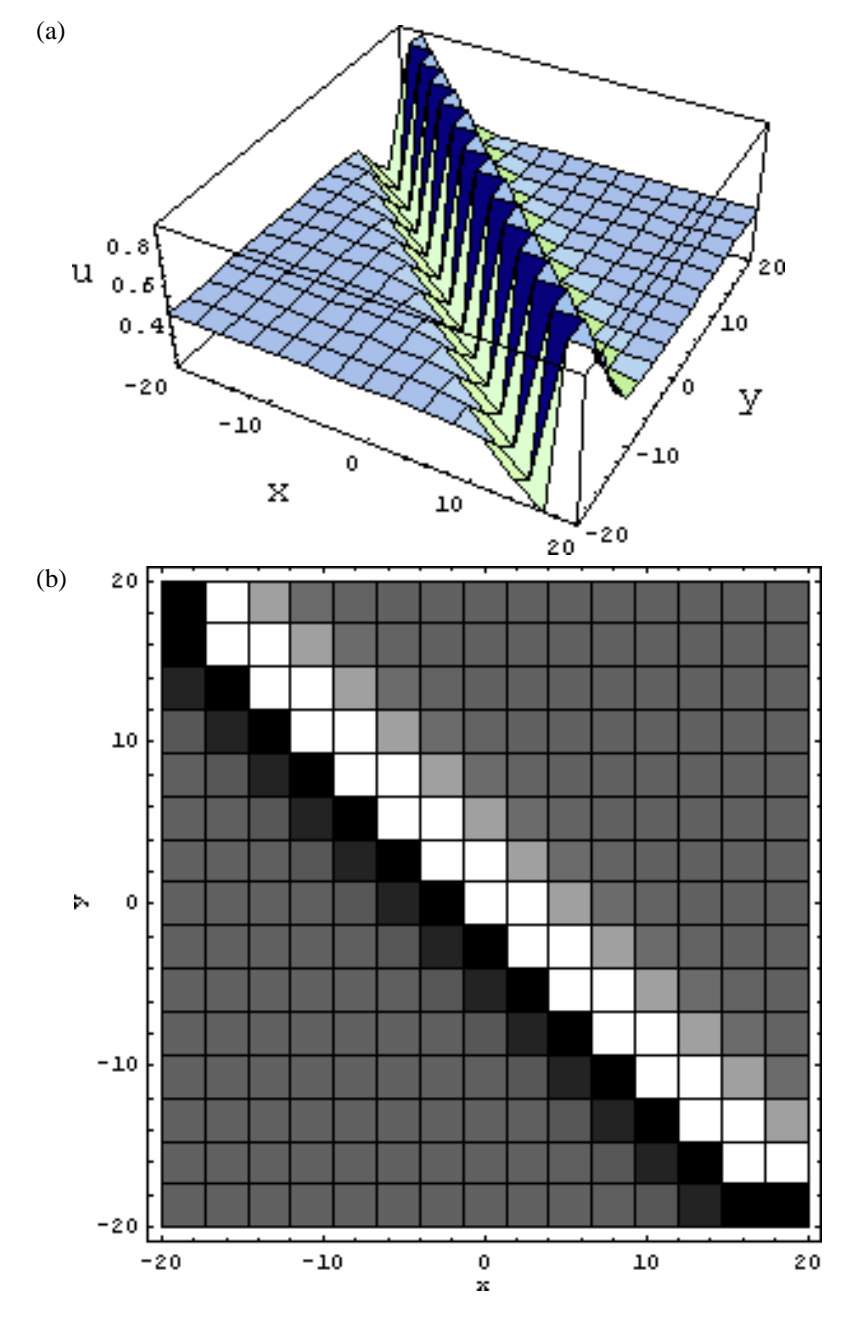


Fig. 4. (a) Plot of the concentration u(x,y), where  $a_0 + b_0 = 1/2$ , for D = 0.25, L = 0.1, v = 0.5, and k = -0.1. (b) Density plot of the concentration u(x,y), where  $a_0 + b_0 = 1/2$ , for D = 0.25, L = 0.1, v = 0.5, and k = -0.1.

From (49), it is clear that for the case k < 0 we get

$$u(x,y,t) = a_0 + \frac{D}{Lv}\sqrt{-k} \coth[\sqrt{-k}\zeta],$$
where  $\zeta = x + y + \lambda t$  and  $\lambda = Lv(-1 + 2a_0)$ , (54)

while for k > 0 it is

$$u(x, y, t) = a_0 - \frac{D}{Lv} \sqrt{k} \cot[\sqrt{k}\zeta],$$
where  $\zeta = x + y + \lambda t$  and  $\lambda = Lv(-1 + 2a_0)$ , (55)

and k and  $a_0$  are arbitrary constants. Finally, (50) leads for k < 0 to

$$u(x,t) = a_0 + \frac{D}{Lv}\sqrt{-k}\left\{\coth\left[\sqrt{-k}\zeta\right] + \tanh\left[\sqrt{-k}\zeta\right]\right\},\,$$

where 
$$\zeta = x + y + \lambda t$$
 and  $\lambda = Lv(-1 + 2a_0)$ , (56)

and

$$u(x,t) = a_0 + \frac{D}{Lv} \sqrt{k} \{ \cot[\sqrt{k}\zeta] - \tan[\sqrt{k}\zeta] \},$$
where  $\zeta = x + y + \lambda t$  and  $\lambda = Lv(-1 + 2a_0)$ , (57)

for k > 0, where  $a_0$  is an arbitrary constant.

### 4. Discussion

The travelling wave solutions derived in this paper include soliton, periodical, rational and singular solutions. Now, let us consider certain interesting types of the obtained solutions. An interesting solution for the case (i) is given by (38):

$$u(x,y,t) = \left[\frac{D\sqrt{-k}}{vL(m-1)} \left(\pm 1 - \tanh[\sqrt{-k}\zeta]\right)\right]^{\frac{1}{m-1}},$$
  
where  $\zeta = x + y + \lambda t$  and  $\lambda = \frac{\mp 2D\sqrt{-k}}{m-1}$ ,

which is applicable for any value of m where  $m \neq 0$ 

and 1. This solution is a kink-type solitary wave solution and its typical behavior is depicted in Figure 2. As shown from the density plot in Fig. 3, it is obvious that the presence of an obstacle, whether stationary or moving, in a driven diffusive flow with nonlinear drift will distort the local concentration profile to a state which divides the (x,y)-plane into two regions about the straight line  $x+y+\lambda\,t=0$  (not as expected about the strip axis x=0). The concentration is relatively higher at one side than at the other side, apart from the value of  $\frac{D}{vL}$ . Also, it is clear that the concentration u(L) (for m>1) as a function of the obstacle length L approaches zero as L approaches infinity. Also, another interesting solution for the case (ii) is given by (51) which in the stationary state (taking  $a_0+b_0=\frac{1}{2}$ ) becomes

$$u(x,y) = \frac{1}{2} + \frac{D}{Lv}\sqrt{-k}\tanh[\sqrt{-k}(x+y)].$$

It is also a kink-type solitary wave solution and resembles the same characterisics as the previous one but in this case the presence of the obstacle will divide the (x,y)-plane into two regions about the straight line x+y=0.

Finally, solutions of the type (56) develope a singularity at a finite point and in such a case the concentration profile is nonuniform as depicted in Figure 4.

- [1] A. Rosato, F. Prinz, K. J. Strandburg, and R. H. Swendsen, Powder Technol. **49**, 59 (1986).
- [2] A. Rosato, K. J. Strandburg, F. Prinz, and R. H. Swendsen, Phys. Rev. Lett. **58**, 1038 (1987).
- [3] F. J. Alexander and J. L. Lebowitz, J. Phys. A: Math. Gen. 23, L375 (1990).
- [4] F. J. Alexander and J. L. Lebowitz, J. Phys. A: Math. Gen. 27, 683 (1994).
- [5] J. R. Philip, J. H. Knight, and R. T. Waechter, Water Resources Res. 25, 16 (1989).
- [6] C. Knessl and J. B. Keller, J. Math. Phys. 38, 267 (1997).
- [7] E. A. Saied and R. G. Abd El-Rahman, J. Stat. Phys. 94, 2253 (1999).
- [8] S. A. Elwakil, S. K. El-Labany, M. A. Zahran, and R. Sabry, Phys. Lett. A 299, 179 (2002).

- [9] S. A. Elwakil, S. K. El-Labany, M. A. Zahran, and R. Sabry, Chaos, Solitons, Fractals 17, 121 (2003).
- [10] S. A. Elwakil, S. K. El-Labany, M. A. Zahran, and R. Sabry, Z. Naturforsch. 58a, 39 (2003).
- [11] P.J. Olver, Applications of Lie Groups to Differential Equations, Springer, Berlin 1986.
- [12] G. W. Bluman and S. Kumei, Symmetries and Differential Equations, Springer, Berlin 1989.
- [13] S. K. El-Labany, A. M. Elhanbaly, and R. Sabry, J. Phys. A: Math. Gen. 35, 8055 (2002).
- [14] V. V. Gudkov, J. Math. Phys. 38, 4794 (1997).
- [15] E. Fan, Phys. Lett. A 282, 18 (2001).
- [16] E. Fan, J. Phys. A: Math. Gen. 35, 6853 (2002).
- [17] B. Li, Y. Chen, and H. Zhang, J. Phys. A: Math. Gen. 35, 8253 (2002).